Global and network functional connectivity of Nucleus Basalis of Meynert is strengthened in blind individuals

Ji Won Bang[1*], Russell W. Chan[1], Carlos Parra[1], Matthew, C. Murphy[2-3], Joel S. Schuman[1,4-6], Amy C. Nau[3,7], Kevin C. Chan[1,3-6,8*]

[1]Department of Ophthalmology, NYU Grossman School of Medicine, NYU Langone Health, New York University, New York, New York, USA.

[2]Department of Radiology, Mayo Clinic, Rochester, Minnesota, USA.

[3]Department of Ophthalmology, School of Medicine, University of Pittsburgh, Pittsburgh, PA, USA.

[4]Neuroscience Institute, NYU Grossman School of Medicine, NYU Langone Health, New York University, New York, New York, USA.

[5]Center for Neural Science, College of Arts and Science, New York University, New York, New York, USA.

[6]Department of Biomedical Engineering, Tandon School of Engineering, New York University, New York, New York, USA.

[7]Korb and Associates, Boston, Massachusetts, USA.

[8]Department of Radiology, NYU Grossman School of Medicine, NYU Langone Health, New York University, New York, New York, USA.

*Co-Correspondence to:

Ji Won Bang, Ph.D.
222 E 41st Street, Room 360
Department of Ophthalmology
NYU Grossman School of Medicine
NYU Langone Health
New York University, New York, NY, USA 10017
Tel: (929) 455-5049 Fax: (212) 263-8749
Email: JiWon.Bang@nyulangone.org

and

Kevin C. Chan, Ph.D.
222 E 41st Street, Room 362
Departments of Ophthalmology and Radiology
NYU Grossman School of Medicine
NYU Langone Health
New York University, New York, NY, USA 10017
Tel: (212) 263-7602 Fax: (212) 263-8749
Email: chuenwing.chan@fulbrightmail.org

Total number of figures/tables: 5 figures/1 table

Acknowledgments

We would like to thank Jacqueline Fisher, and Mark Vignone for their help with subject recruitment and technical support. This work is supported in part by the National Institutes of Health R01-EY028125 (Bethesda, Maryland), United States Department of Defense W81XWH2110615 (Arlington, Virginia), BrightFocus Foundation G2021001F (Clarksburg, Maryland), and an unrestricted grant from Research to Prevent Blindness to NYU Langone Health Department of Ophthalmology (New York, New York).

Declaration of Conflicting Interests

The authors declare no conflict of interests.

Abstract

Vision loss causes dramatic changes in brain function which are thought to facilitate behavioral adaptation. One interesting prospect is that the cholinergic signals are involved in this blindness-induced plasticity. Critically, the nucleus basalis of Meynert is the principal source of the cholinergic signals, however, no studies have yet investigated whether the nucleus basalis of Meynert is altered in blindness. Therefore, here we examined its structure, cerebrovascular response, and the resting-state functional connectivity in blind individuals. We found that the global signal of the nucleus basalis of Meynert as well as its network connectivity with the visual, language, and default mode network is significantly enhanced in early blind individuals. On the other hand, its structure and cerebrovascular response remain unchanged in early blind individuals. Further, we observed that less visual experience predicts stronger global and network connectivity of the nucleus basalis of Meynert. These results suggest that the nucleus basalis of Meynert develops a stronger neuromodulatory influence on the cortex of blind individuals at both global and network levels.

Keywords: nucleus basalis of Meynert, blindness, global connectivity, network connectivity, resting-state, fMRI, plasticity, choline, plasticity

Introduction

The brain retains a profound amount of plasticity which enables us to adapt to environmental demands (Bang and others 2021; Bruel-Jungerman and others 2007). Particularly, loss of vision has been a critical model for investigating brain plasticity. Ample amount of evidence indicates that blind individuals perform better than sighted people at various non-visual tasks including echolocation (Lessard and others 1998; Voss and others 2004), pitch discrimination (Gougoux and others 2004), speech discrimination (Niemeyer and Starlinger 1981), verbal memory (Amedi and others 2003; Hull and Mason 1995) and tactile discrimination (Goldreich and Kanics 2003; Van Boven and others 2000).

One of the influential mechanisms proposed to explain this superior ability of blind individuals is that compensatory alterations occur in the brain which enhance the processing of non-visual input (Fine and Park 2018). Indeed, compelling evidence indicates that the blind individuals' visual cortex becomes recruited for a wide range of non-visual tasks such as Braille reading (Burton and others 2002; Kupers and others 2007; Sadato and others 1996), auditory localization (Norman and Thaler 2019; Voss and others 2006), sensory substitution tasks (Murphy and others 2016; Nau and others 2015; Ptito and others 2005; Striem-Amit and others 2012), verbal memory (Amedi and others 2003), language (Bedny and others 2011; Bedny and others 2015), and mathematics (Amalric and others 2018; Kanjlia and others 2019). When the visual cortex was disrupted by transcranial magnetic stimulation during the task, the performance was impaired in blind individuals (Merabet and others 2009). Beyond the visual cortex, the left superior temporal sulcus, and the fusiform area were shown to be activated to a greater extent during voice

104 discrimination in congenitally blind individuals (Gougoux and others 2009). This line of studies
105 suggests that the cortical functional reorganization occurs in blindness that may modulate
106 various behavioral adaptations.
107
108 In particular, cholinergic signals have been suggested to play a role in blindness-induced
109 compensatory alterations. The nucleus basalis of Meynert (NBM) provides the major source of
110 cholinergic signals to the cortex. The cholinergic input from NBM innervates diffusively the
111 cortex including both primary sensory areas and high-order association areas (Mesulam and
112 others 1983; Mesulam and others 1984). Critically, the cholinergic signals are involved in
113 attention (Everitt and Robbins 1997; Sarter and others 2005) and experience-dependent
114 cortical plasticity (Bakin and Weinberger 1996; Froemke and others 2007; Kilgard and
115 Merzenich 1998). In addition, the cholinergic neurons in NBM are known to rapidly modulate
116 sensory processing (Goard and Dan 2009; Pinto and others 2013). For example, when NBM is
117 stimulated electrically or optogenetically, the cortical coding of visual information in V1 is
118 enhanced (Goard and Dan 2009; Pinto and others 2013) and the performance on a visual task is
119 improved in animals (Pinto and others 2013).
120
121 Relatedly, the input from NBM is thought to play a key role in orchestrating spontaneous
122 activity across the brain (Turchi and others 2018). The resting-state fMRI provides a useful
123 platform to investigate spontaneous brain activity. This spontaneous brain activity is
124 distinguishable into two qualitatively different signals. The first one is a network signal that is a
125 specific correlation between different brain areas. This network signal reflects the functionally

126 connected network architecture (Damoiseaux and others 2006). Further, studies showed that
127 this network signal is constrained by large-scale anatomical connections (Hagmann and others
128 2008; Honey and others 2009). On the other hand, global signal refers to broadly shared signal
129 across the neocortex (Scholvinck and others 2010). This global signal is suggested to reflect
130 large-scale coordination of brain activity (Cole and others 2010). Building on this, a recent study
131 demonstrated that NBM regulates global signal fluctuations (Turchi and others 2018).
132 Specifically, when NBM was inactivated, the global signal components ipsilateral to the
133 injection site were suppressed whereas the specific correlations that define resting-state
134 networks were unaffected. This finding suggests that the input of NBM contributes to the
135 global signals but has little influence on the network signals.
136
137 In the field of blindness-induced plasticity, the amount of choline was observed to be higher in
138 the visual cortex of early blind individuals (Coullon and others 2015; Weaver and others 2013).
139 An interesting question arises from this observation, namely, whether NBM plays a causal role
140 in enhancing the cholinergic signals in the blind's visual cortex. This idea is supported by the
141 fact that NBM sends cholinergic projections to the entire cortex including visual areas
142 (Mesulam and others 1983; Mesulam and others 1984).
143
144 Here, we propose that NBM develops a stronger influence to the neocortex of blind individuals
145 in order to facilitate non-visual processing. Using anatomical MRI and resting-state functional
146 MRI, we provide novel support for this prediction, presenting enhanced global and network
147 connectivity of NBM during rest in early blind individuals. Particularly, the cortical networks

that present increased network connectivity with NBM include visual networks bilaterally (occipital visual cortex, lateral visual cortex, medial visual cortex), language networks of the left hemisphere (inferior frontal gyrus (IFG), posterior superior temporal gyrus (pSTG)), and default mode network (posterior cingulate cortex (PCC)). We further confirmed that these changes in the network and global connectivity of NBM in early blind individuals are not affected by the structural or cerebrovascular changes of NBM. While these alterations of the network connectivity, as well as global connectivity, are significant only within the early blind individuals, the years of visual experience predict both network and global connectivity among early blind, late blind individuals, and sighted controls. These results suggest that NBM may develop stronger cholinergic innervations onto the cortex to support behavioral adaptation in blind individuals.

Materials and Methods

Participants

Forty-nine subjects (29 females, mean age 54.67 ± 2.12) without any history of neurological disorders participated in the study. Seven subjects were congenitally blind, sixteen subjects were late-blind individuals, and twenty-six subjects were sighted controls. One among late blind individuals was later excluded from the entire analysis because the functional MR scan failed to cover NBM. Additional one early blind individual was excluded from the rCVR analysis due to a problem in rCVR computation but included for other analyses. The demographic data of the early and late blind individuals are depicted in Table 1. Age and gender were not significantly different across three groups (age: $F(2,45)=0.118$, $P=0.889$, partial $\eta^2=0.005$, one-way ANOVA; gender: $\chi^2(2)=0.614$, $P=0.736$, Phi=0.113, Pearson Chi-Square test). This study was approved by the Institutional Review Board of the University of Pittsburgh. All subjects provided written informed consent.

Gender	Age (years)	Onset age (years)	Duration of blindness (years)	Cause
M	58	51	7	Traumatic accident
F	59	53	6	Congenital cataracts, aniridia, pediatric glaucoma
F	53	28	25	diabetic retinopathy
M	62	51	11	Traumatic accident
F	64	0	64	congenital
M	25	0	25	congenital
F	58	0	58	congenital
F	35	31	4	Traumatic accident
M	55	35	20	Trauma accident
M	56	0	56	congenital
M	58	7	51	encephalitis
F	58	46	12	glaucoma
M	18	13	5	pigmentosa
F	60	0	60	retinopathy of prematurity
F	62	0	62	congenital
F	71	59	12	glaucoma
F	60	31	29	glaucoma
M	75	59	16	pigmentosa
F	39	17	22	retinopathy of prematurity
F	30	23	7	tumors
M	63	0	63	retinopathy of prematurity
M	64	54	10	detached retinas

Table 1. Subject demographic and clinical information

MRI data acquisition

MRI data were collected with a 3 T Siemens Allegra MR scanner. Anatomical MR images were obtained using a T1-weighted MPRAGE (176 contiguous 1-mm sagittal slices, voxel size = 1×1×1 mm^3, repetition time (TR) = 1400 ms, echo time (TE) = 2.5 ms, field of view (FOV) = 256×256 mm^2, flip angle = 8°, acquisition matrix = 256×256). Functional images were obtained using a single-shot gradient-echo echo-planar imaging (EPI) sequence (36 contiguous 3-mm axial slices,

184 voxel size = 2×2×3 mm^3, TR = 2000 ms, TE = 25 ms, FOV = 205×205 mm^2, acquisition matrix =
185 64×64) while subjects were at rest with eyes closed. The slices covered the whole brain.
186
187 MRI Voxel-based morphometry (VBM) analysis
188 We conducted VBM analysis to test whether NBM presents any atrophy within the grey and
189 white matter. T1-weighted MRI images were segmented and normalized to MNI space using
190 SPM12 (http://www.fil.ion.ucl.ac.uk/spm/). Then, the images were smoothed using a Gaussian
191 kernel of 6mm FWMH.
192
193 Resting-state fMRI analysis
194 T1-weighted MRI and resting-state fMRI images were preprocessed using CONN's default MNI
195 pipeline in CONN toolbox, version 18.a (www.nitrc.org/projects/conn,RRID:SCR_009550)
196 (Whitfield-Gabrieli and Nieto-Castanon 2012). The default preprocessing steps included the
197 functional realignment and unwarping, slice-timing correction, functional outlier detection,
198 functional segmentation and normalization, structural segmentation and normalization,
199 functional smoothing using a Gaussian kernel of 8mm FWMH. The noise components from
200 cerebral white matter, cerebrospinal fluid, estimated subject-motion parameters, scrubbing,
201 and linear session effects were removed from the functional images for each voxel and each
202 subject using an anatomical component-based noise correction procedure (aCompCor)
203 implemented in CONN's default de-noising pipeline. The functional images were then band-
204 pass filtered to 0.008 Hz – 0.09 Hz.
205

The map of NBM on MNI space was obtained from SPM Anatomy toolbox version 3.0 (Zaborszky and others 2008). In particular, this NBM map was created based on stereotaxic probabilistic maps of the basal forebrain. Magnocellular cell groups in the subcommissural-sublenticular region of the basal forebrain were delineated and then warped to the MNI space (Zaborszky and others 2008). The functional connectivity of the seed NBM was then computed using CONN toolbox. For global correlation analysis, we calculated the average of correlation coefficients between each voxel and the rest voxels of the brain across time series. Then we extracted the global correlation coefficients from the voxels corresponding to seed NBM and averaged them across the seed voxels to identify NBM's brain-wide correlation properties. For ROI-level analysis, we used 30 cortical networks that CONN generated. These include default mode network (bilateral lateral parietal cortex, medial prefrontal cortex, posterior cingulate cortex), dorsal attention network (bilateral frontal eye fields, bilateral intraparietal sulcus), frontoparietal network (bilateral lateral prefrontal cortex, bilateral posterior parietal cortex), language network (bilateral inferior frontal gyrus, bilateral posterior superior temporal gyrus), salience network (anterior cingulate cortex, bilateral anterior insular cortex, bilateral rostral prefrontal cortex, bilateral supramarginal gyrus), sensorimotor network (bilateral lateral sensorimotor cortex, superior sensorimotor cortex), and visual network (bilateral lateral visual cortex, medial visual cortex, occipital visual cortex). We computed the correlation coefficients between the seed NBM and all 30 cortical networks and converted them to z-value using Fisher's r-to-z transformation (Lowe and others 1998). For voxel-level analysis, the correlation coefficients were obtained between the seed NBM and each voxel and were converted to z-value using Fisher's r-to-z transformation.

228

229 rCVR analysis

230 rCVR maps were obtained from the resting-state fMRI images using MriCloud

231 (https://mricloud.org/). Following prior methods (Liu and others 2017), we computed the voxel-

232 wise CVR index (α) using a general linear model between normalized BOLD time series

233 (ΔBOLD/BOLD) and the global signal time series (*GS*). Then we calculated the voxel-wise rCVR

234 by normalizing α by tissue signal intensity averaged across the whole brain (SI). The residuals

235 term (β) was not used for analysis. Below is the summary of these steps.

236 $\text{rCVR} = \frac{\alpha}{\text{SI}}$ where α is obtained from $\frac{\Delta\text{BOLD}}{\text{BOLD}} = \alpha \bullet \text{GS} + \beta$

237

238 We extracted rCVR values from NBM and 30 cortical networks which are in MNI space.

239

240 Statistics

241 For all statistical analyses, we used two-tailed parametric tests with statistical significance set at

242 $P<0.05$. We assessed the assumption of sphericity for all measures ANCOVAs using Mauchly's

243 sphericity tests. When the assumption of sphericity was violated, we reported Huynh-Feldt

244 corrected results. In the following post-hoc tests, we used Bonferroni method to correct the

245 multiple comparisons and reported Bonferroni-corrected P values. For whole-brain voxel-level

246 analysis, a voxel height threshold of $p<0.001$ and a cluster height threshold of p-FDR

247 corrected<0.05 were used.

248

249 Data Availability

250 The global and network connectivity, rCVR, and the structural volume data are freely available

251 at https://osf.io/axy45/.

252

253

Results

We first examined whether the white and grey matter of NBM (**Fig. 1A**) are altered in blindness using VBM analysis. For this, we applied a one-way ANCOVA with a factor group (control, early blind, late blind) to the white and grey matter volumes of NBM as controlling for total intracranial volume and age. The results revealed no significant main effect of group for both white and grey matter (white matter volume: $F(2,43)=1.705$, $P=0.194$, partial $\eta^2=0.073$; grey matter volume: $F(2,43)=1.063$, $P=0.354$, partial $\eta^2=0.047$), suggesting that the anatomical structure of NBM remains intact in blindness.

Next, we investigated whether NBM presents enhanced global signals in blind individuals. To test for this effect, we computed the global connectivity between NBM and all other cortical voxels. Then, we conducted a one-way ANCOVA with a factor group (control, early blind, late blind) controlling for age. The results showed a significant main effect of group ($F(2,45)=3.530$, $P=0.038$, partial $\eta^2=0.136$; **Fig. 1B**). Further post-hoc tests showed that the early blind group has significantly greater global connectivity compared to sighted controls (control vs. early blind, $P=0.034$, 95% CI=-1.814 – -0.055). However, this increased global connectivity of NBM in the early blind group did not differ from that in the late blind group (early blind vs. late blind, $P=0.248$, 95% CI=-0.268 – 1.605; control vs. late blind, $P=0.957$, 95% CI=-0.923 – 0.391). Further, we examined whether the global connectivity of NBM is associated with the years of visual experience by conducting a partial correlation analysis controlling for age. The results showed that less visual experience predicts a stronger global signal of NBM ($r=-0.453$, $p=0.001$; **Fig. 1C**).

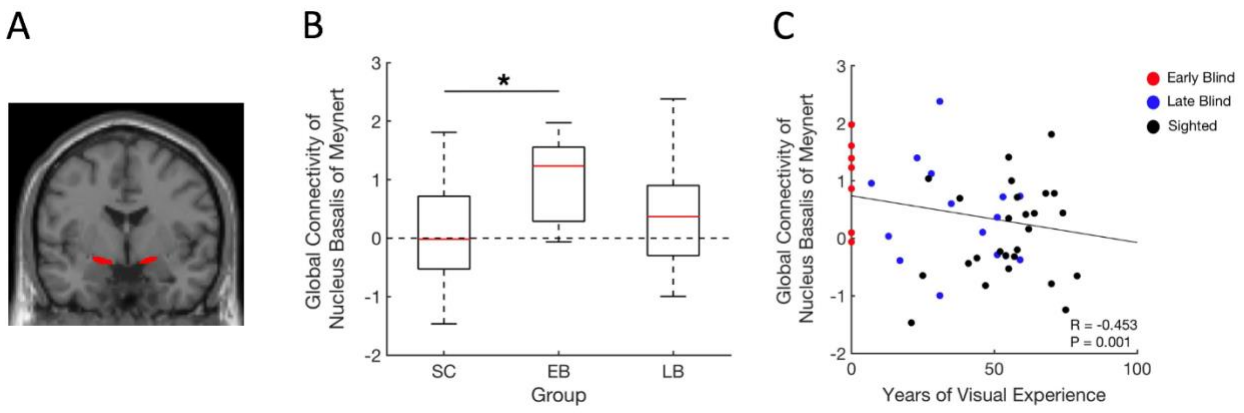

Fig. 1. The Nucleus Basalis of Meynert. (A) Coronal view of the nucleus basalis of Meynert. (B) Global connectivity between the nucleus basalis of Meynert and the entire cortical areas is significantly increased in the early blind group compared to sighted controls. The distributions are represented using box plots. "SC", "EB," and "LB" refer to the sighted controls, early blind and late blind groups. * Bonferroni-corrected $P < 0.05$. (C) Years of visual experience predict global connectivity of nucleus basalis of Meynert. Each point represents one subject. Red, blue and black colors indicate early blind, late blind, and sighted controls. The R and P values in the figure refer to the result of a partial correlation test between years of visual experience and global connectivity of nucleus basalis of Meynert controlling for age. N=48.

Having confirmed the enhanced global signal of NBM in early blind individuals, we further examined whether early blind individuals have increased network connectivity as well. We addressed this question using ROI- and voxel-based analyses. For ROI-based analysis, we created 30 cortical network ROIs (see Materials and Methods) and computed the functional connectivity between NBM and each of the network ROIs. We then conducted a two-way mixed measures ANCOVA with factors group (control, early blind, late blind) and network (30 cortical networks) to the functional connectivity controlling for age. The results revealed a significant main effect of group ($F(2,44)=9.339$, $P<0.001$, partial $\eta^2=0.298$) and significant interaction between group and network ($F(58,1276)=1.754$, Huynh-Feldt correction, $P=0.015$, partial $\eta^2=0.074$) but no main effect of network ($F(29,1276)=0.952$, $P=0.494$, partial $\eta^2=0.021$). Following post-hoc tests showed that the functional connectivity of the early blind individuals is

298 greater than that of the sighted controls and late blind individuals (control vs. early blind:
299 P<0.001, 95% CI=-0.160 – -0.043; control vs. late blind: P=0.760, 95% CI=-0.065 – 0.024; early
300 blind vs. late blind: P=0.008, 95% CI=0.018 – 0.143). Further, a significant interaction between
301 group and network suggests that the functional connectivity changes across the group and that
302 this pattern of change differs across networks.
303
304 Given the significant interaction between group and network, we examined more in detail how
305 the functional connectivity changes across networks by conducting a one-way ANCOVA with a
306 factor group (control, early blind, late blind) to each network as controlling for age. The results
307 revealed a significant main effect of group at visual networks bilaterally (occipital visual cortex:
308 $F(2, 44)=5.491$, P=0.007, partial $\eta^2=0.200$; left lateral visual cortex: $F(2, 44)=8.853$, P=0.001,
309 partial $\eta^2=0.287$; right lateral visual cortex: $F(2, 44)=10.818$, P<0.001, partial $\eta^2=0.330$; medial
310 visual cortex: $F(2, 44)=9.861$, P<0.001, partial $\eta^2=0.310$; **Fig. 2B**), language networks of the left
311 hemisphere (left posterior superior temporal gyrus: $F(2, 44)=10.413$, P<0.001, partial $\eta^2=0.321$;
312 left inferior frontal gyrus: $F(2, 44)=8.105$, P=0.001, partial $\eta^2=0.269$; **Fig. 2B**), and default mode
313 network (posterior cingulate cortex: $F(2, 44)=5.245$, P=0.009, partial $\eta^2=0.193$; **Fig. 2B**).
314 Following post-hoc tests showed that in the occipital visual cortex, the early blind group has
315 higher functional connectivity compared to sighted controls (control vs. early blind: P=0.006,
316 95% CI=-0.441 – -0.060; control vs. late blind: P=0.542, 95% CI=-0.224 – 0.066; early blind vs.
317 late blind: P=0.129, 95% CI=-0.033 – 0.376). In the left lateral visual cortex, the functional
318 connectivity of the early blind group is higher than that of the sighted controls and late blind
319 group (control vs. early blind: P<0.001, 95% CI=-0.465 – -0.117; control vs. late blind: P=0.236,

95% CI=-0.229 – 0.037; early blind vs. late blind: P=0.040, 95% CI=0.007 – 0.383). Similar post-hoc results, that is significantly increased functional connectivity of the early blind group compared to that of the sighted controls and late blind group were observed in the right lateral visual cortex (control vs. early blind: P<0.001, 95% CI=-0.533 – -0.155; control vs. late blind: P=0.083, 95% CI=-0.276 – 0.012; early blind vs. late blind: P=0.039, 95% CI=0.008 – 0.416), medial visual cortex (control vs. early blind: P<0.001, 95% CI=-0.492 – -0.138; control vs. late blind: P=0.389, 95% CI=-0.219 – 0.051; early blind vs. late blind: P=0.013, 95% CI=0.041 – 0.422), left posterior superior temporal gyrus (control vs. early blind: P<0.001, 95% CI=-0.421 – -0.119; control vs. late blind: P=0.098, 95% CI=-0.218 – 0.013; early blind vs. late blind: P=0.041, 95% CI=0.005 – 0.331), left inferior frontal gyrus (control vs. early blind: P=0.002, 95% CI=-0.373 – -0.75; control vs. late blind: P=1.000, 95% CI=-0.097 – 0.131; early blind vs. late blind: P=0.002, 95% CI=0.081 – 0.402), and posterior cingulate cortex (control vs. early blind: P=0.008, 95% CI=-0.359 – -0.044; control vs. late blind: P=1.000, 95% CI=-0.134 – 0.107; early blind vs. late blind: P=0.026, 95% CI=0.018 – 0.357).

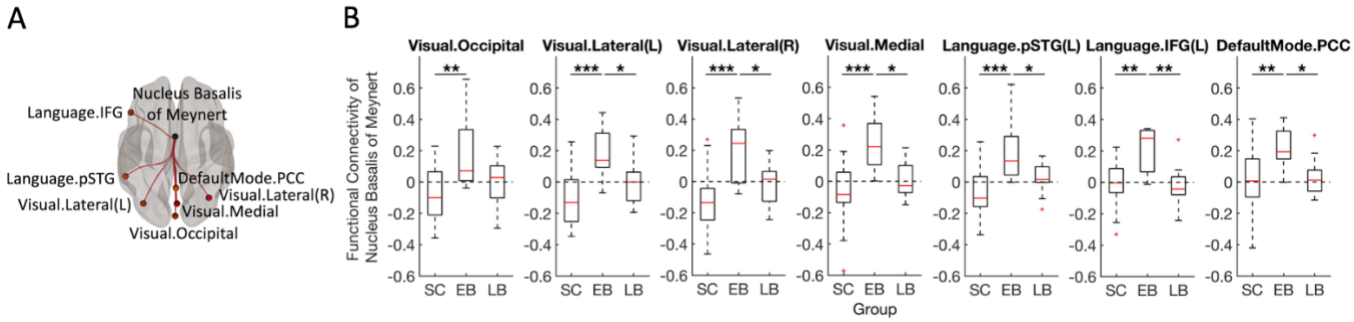

Fig. 2. Early blind individuals have increased functional connectivity between nucleus basalis of Meynert and cortical networks including visual networks, language networks, and default mode network. (A) Schematic depiction of the nucleus basalis of Meynert and seven cortical networks (occipital, lateral, medial visual cortices, left posterior superior temporal gyrus, left inferior frontal gyrus, posterior cingulate cortex) which showed enhanced connectivity with the nucleus basalis of Meynert in the early blind group. (B) Functional connectivity between the nucleus basalis of Meynert and seven cortical networks. The distributions are represented using box

plots and the outliers are plotted as plus signs. “SC”, “EB,” and ”LB” refer to the sighted controls, early blind and late blind groups. * Bonferroni-corrected $P < 0.05$, ** Bonferroni-corrected $P < 0.01$. N=48.

The above analyses were conducted on averaged functional connectivity across large-scale brain networks. For completeness, we also examined the functional network connectivity of NBM at the voxel level. For this, we computed the functional connectivity between NBM and each cortical voxel. We then conducted a one-way ANCOVA with a factor group (control, early blind, late blind) controlling for age. As in the above ROI-level analysis, we observed a significant main effect of group within the visual cortex bilaterally, and the left middle temporal gyrus (**Fig. 3A**). Additionally, the voxel-level analysis found group difference in the bilateral fusiform area, which was previously included in the medial visual network during the ROI-level analysis. Further post-hoc tests (**Fig. 3B**) revealed that this group difference was driven by the early blind group. A comparison between early blind and sighted controls revealed that early blind individuals have greater functional connectivity of NBM at the visual cortex bilaterally, and left superior, middle, inferior temporal gyrus, as well as fusiform area bilaterally. Another comparison between early and late blind groups showed that the early blind group has significantly higher connectivity of NBM at the right visual cortex. On the other hand, late blind and sighted controls did not yield a significant difference at any voxels. These results replicate the ROI-level analysis results although the voxel-level analysis did not observe significant changes within the left inferior frontal gyrus (language network) and the posterior cingulate cortex (default mode network), possibly due to multiple comparisons correction at the voxel level.

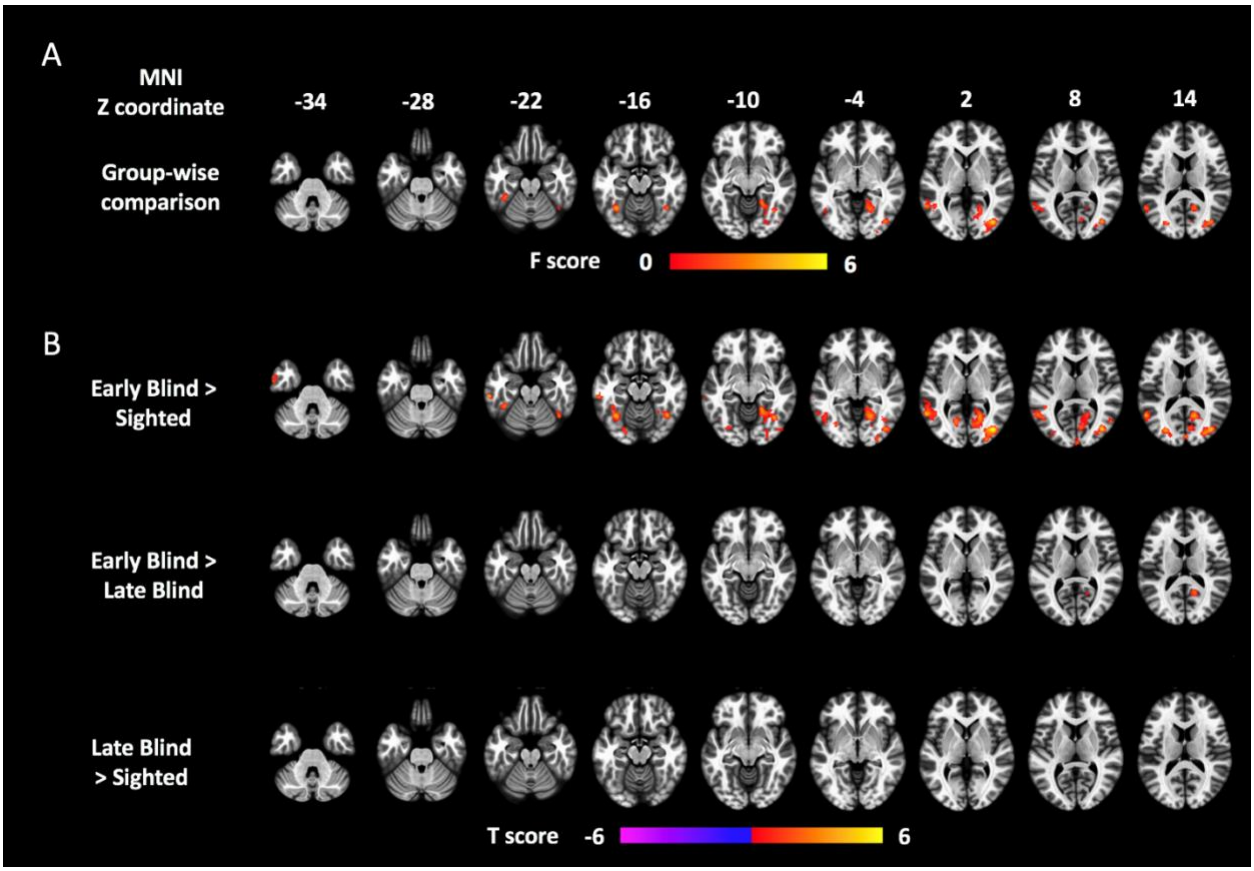

Fig. 3. Group difference of functional connectivity of the nucleus basalis of Meynert. (A) F map for the group-wise difference. Significant group differences are observed in the bilateral visual cortex, left middle temporal gyrus, and bilateral fusiform area. (B) Post-hoc group-wise t-tests between groups. The early blind individuals have increased connectivity of nucleus basalis of Meynert within the bilateral visual cortex, left superior, middle, inferior temporal gyrus, and the bilateral fusiform area compared to sighted controls. Another comparison between early and late blind individuals shows that the early blind group has higher connectivity in the right visual cortex. The late blind and sighted individuals did not show any significant difference. N=48

Since the voxel-level results replicate the findings of the ROI-level analysis, we further explored whether the increase of functional connectivity between NBM and cortical networks is negatively associated with the years of visual experience. For this, we conducted partial correlation analyses controlling for age, using six cortical networks which showed enhanced connectivity with NBM in the early blind group. The results revealed significant correlations

within visual networks (occipital visual network: r=-0.452, p=0.001; left lateral visual network: r=-0.548, p<0.001; right lateral visual network: r=-0.568, p<0.001; medial visual network: r=-0.555, p<0.001), language networks (left posterior superior temporal gyrus: r=-0.527, p<0.001; left inferior frontal gyrus: r=-0.389, p=0.007), and default mode network (posterior cingulate cortex: r=-0.386, p=0.007; **Fig. 4**). The results indicate that less visual experience predicts greater functional connectivity of NBM within these networks.

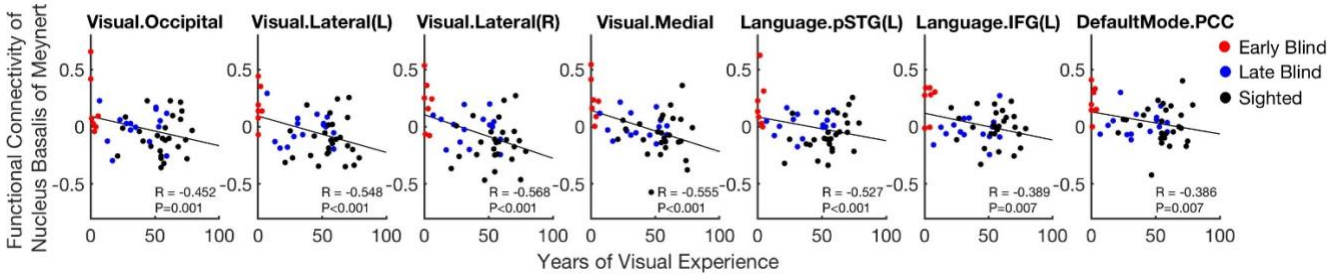

Fig. 4. Years of visual experience predict functional connectivity of nucleus basalis of Meynert. Significant correlations were observed within visual networks (occipital, lateral, medial visual areas), language networks (left posterior superior temporal gyrus, left inferior frontal gyrus), and default mode network (posterior cingulate cortex). Each point represents one subject. Red, blue and black colors indicate early blind, late blind, and sighted controls. For visualization purposes, early-blind data points are plotted apart from each other although their x values are all 0. The R and P values in the figure refer to the results of partial correlation tests between years of visual experience and functional connectivity of nucleus basalis of Meynert controlling for age. N=48.

Finally, we examined whether these global and network signals are affected by cerebrovascular changes using the relative cerebrovascular reactivity (rCVR) map computed from resting-state fMRI (see Materials and Methods). The rCVR measures the cerebral blood vessels' ability to dilate or constrict in response to vasoactive stimuli (Liu and others 2019). Since the BOLD signals in the resting-state fMRI are tightly related to the degree to which cerebral blood

vessels respond to the neurovascular coupling chemical signals (Gauthier and Fan 2019), it is important to examine whether the observed resting-state functional connectivity changes in the early blind group are influenced by cerebrovascular changes. To test whether there are any alterations of rCVR within NBM and the cortical networks that showed significant changes in the early blind group, we applied a one-way ANCOVA with a factor group (control, early blind, late blind) to the rCVR measures controlling for age. We observed no significant main effect of group in NBM ($F(2, 43)=0.257$, $P=0.775$, partial $\eta^2=0.012$), left lateral visual cortex ($F(2, 43)=2.094$, $P=0.136$, partial $\eta^2=0.089$), and left inferior frontal gyrus ($F(2, 43)=0.417$, $P=0.662$, partial $\eta^2=0.019$; **Fig. 5**). However, significant main effect of group was observed in the occipital visual cortex ($F(2, 43)=4.114$, $P=0.023$, partial $\eta^2=0.161$), right lateral visual cortex ($F(2, 43)=3.235$, $P=0.049$, partial $\eta^2=0.131$), medial visual cortex ($F(2, 43)=3.292$, $P=0.047$, partial $\eta^2=0.133$), left posterior superior temporal gyrus ($F(2, 43)=3.279$, $P=0.047$, partial $\eta^2=0.132$) and posterior cingulate cortex ($F(2, 43)=3.725$, $P=0.032$, partial $\eta^2=0.148$; **Fig. 5**). Further post-hoc tests revealed that this significant main effect of group is driven by the reduced rCVR of the late blind individuals, but not by that of the early blind individuals. Specifically, significant differences between sighted controls and late blind group were observed within the occipital visual cortex ($P=0.020$, 95% CI=0.038 – 0.574), medial visual cortex ($P=0.045$, 95% CI=0.005 – 0.576) and the posterior cingulate cortex ($P=0.029$, 95% CI=0.023 – 0.535; **Fig. 5**) but not within the right lateral visual cortex ($P=0.052$, 95% CI=-0.001 – 0.297) and left posterior superior temporal gyrus ($P=0.220$, 95% CI=-0.031 – 0.207). The results suggest that the late blind individuals have impaired rCVR within the occipital, medial visual cortex, and the posterior cingulate cortex. Critically, comparable rCVRs between early blind individuals and sighted

430 controls suggest that the altered global signal and network connectivity of NBM in early blind
431 individuals are not due to cerebrovascular changes, but rather that these changes are primarily
432 driven by the altered neural activity of NBM.
433

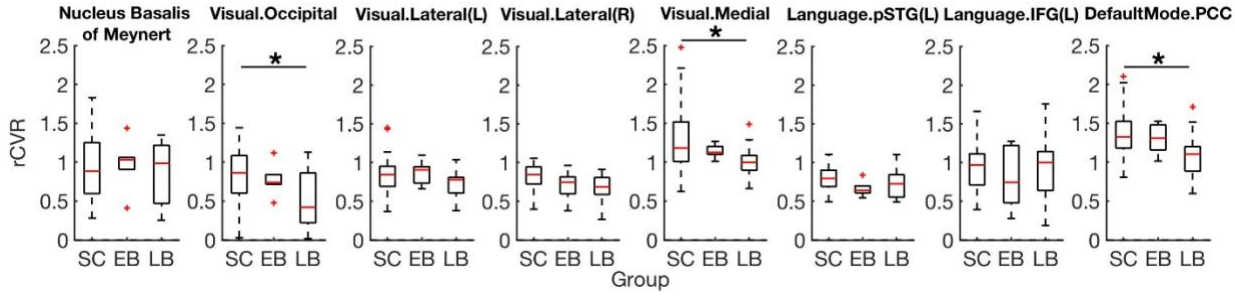

434

435 **Fig. 5.** rCVR of the nucleus basalis of Meynert and seven cortical networks that showed
436 significant change in the early blind group. rCVRs of early blind individuals are comparable to
437 those of sighted controls whereas rCVR of late blind individuals are significantly lower than
438 those of sighted controls within the occipital visual cortex, medial visual cortex, and posterior
439 cingulate cortex. The distributions are represented using box plots and the outliers are plotted
440 as plus signs. “SC”, “EB,” and ”LB” refer to the sighted controls, early blind and late blind
441 groups. * Bonferroni-corrected $P < 0.05$. N=47.
442

443

Discussion

The present results provide robust evidence that spontaneous brain activity of NBM is altered in early blind individuals while its anatomical structure and cerebrovascular response are unchanged. Specifically, we observed that both global and network connectivity of NBM is significantly enhanced in early blind individuals. The cortical networks that present increased connectivity with NBM include bilateral visual networks, language networks of the left hemisphere, and the default mode network. Further, the years of visual experience are significantly correlated with both global and network connectivity among early blind, late blind, and sighted individuals. These results provide direct evidence that NBM develops greater neuromodulatory effects on the neocortex of blind individuals, with its strongest effect on early blind individuals.

The cholinergic innervations originating from NBM are known to play a key role in attention (Everitt and Robbins 1997; Sarter and others 2005), experience-dependent plasticity (Bakin and Weinberger 1996; Froemke and others 2007; Kilgard and Merzenich 1998), and sensory processing (Goard and Dan 2009; Pinto and others 2013). At the scale of seconds, the cholinergic neurons of NBM rapidly modulate the visual processing in V1 (Pinto and others 2013) and the release of choline in the cortex is correlated with behavioral performance (Parikh and others 2007). Thus, our results of enhanced global and network connectivity of NBM suggest that blind individuals are under the greater cholinergic influence which underlies the neural processes of attention, plasticity, and sensory processing. This is consistent with the prior observation that the blind individuals have superior capacity at various non-visual tasks

(Amedi and others 2003; Goldreich and Kanics 2003; Gougoux and others 2004; Lessard and others 1998; Niemeyer and Starlinger 1981) and that their visual cortex is recruited for non-visual information processing (Amalric and others 2018; Amedi and others 2003; Murphy and others 2016; Norman and Thaler 2019; Sadato and others 1996). Indeed, prior studies demonstrated that the visual cortex of early blind individuals contains a greater amount of choline (Coullon and others 2015; Weaver and others 2013).

An important question that arises from our study concerns the role of stronger global connectivity of NBM in blind individuals. The brain region that has high connectivity with the rest of the brain suggests that this area is essential for coordinating large-scale brain activity patterns (Cole and others 2010). Thus, our results suggest that NBM exerts greater influence on coordinating the large-scale brain activity in blind individuals. This explanation is in line with a recent observation that NBM modulates the global signals but has minimal effect on the network connectivity (Turchi and others 2018).

Although NBM was reported to play little role in the network connectivity (Turchi and others 2018), we observed that NBM has increased network connectivity in blind individuals at bilateral visual networks, language networks of the left hemisphere, and the default mode network. Different from global connectivity, the network connectivity contains information about functionally connected brain structure (Damoiseaux and others 2006). Thus, our results indicate that NBM is more functionally coupled with the visual, language, and default mode networks in blind individuals. This enhanced functional connectivity may serve to facilitate

cholinergic modulation during tasks. Indeed, the brain areas that showed increased activity during the non-visual tasks in blind individuals include the visual cortex (Amalric and others 2018; Amedi and others 2003; Bedny and others 2011; Murphy and others 2016; Norman and Thaler 2019; Sadato and others 1996), fusiform area and the left superior temporal sulcus (Gougoux and others 2009). These areas overlap with those that showed increased network connectivity with NBM in the current study. Thus, stronger activation of these cortical areas in blind individuals observed during tasks is likely to be associated with greater cholinergic modulation of NBM.

The current results raise important questions for future studies. First, it remains unclear whether cholinergic signals in the cortical areas are directly driven by NBM activity in blind individuals. This question can be partly addressed by quantifying the amount of choline from the cortex using magnetic resonance spectroscopy and then examining the correlation between the amount of choline and the functional connectivity between NBM and the corresponding cortical areas. Secondly, it has not been explored yet whether the NBM regulates the neural activity in the cortical networks during non-visual tasks in blind individuals. While our results imply such direct regulation of NBM, we only examined the brain activity during rest, but not during the task. If further studies reveal direct modulation of NBM during tasks in blind individuals, its timescales and impact on the performance are the next important questions for future inquiry.

509 To summarize, our results show that the functional connectivity of NBM becomes strengthened
510 in the absence of visual input at both global and network levels. This alteration appears to arise
511 from neural changes of NBM, but not from structural or neurovascular changes. These findings
512 thus suggest that stronger cholinergic modulation of NBM may serve to facilitate behavioral
513 adaptation in blind individuals.
514
515
516
517
518
519

References

Amalric M, Denghien I, Dehaene S. 2018. On the role of visual experience in mathematical development: Evidence from blind mathematicians. Dev Cogn Neurosci 30:314-323.

Amedi A, Raz N, Pianka P, Malach R, Zohary E. 2003. Early 'visual' cortex activation correlates with superior verbal memory performance in the blind. Nat Neurosci 6(7):758-66.

Bakin JS, Weinberger NM. 1996. Induction of a physiological memory in the cerebral cortex by stimulation of the nucleus basalis. Proc Natl Acad Sci U S A 93(20):11219-24.

Bang JW, Hamilton-Fletcher G, Chan KC. 2021. Visual Plasticity in Adulthood: Perspectives from Hebbian and Homeostatic Plasticity. Neuroscientist:10738584211037619.

Bedny M, Pascual-Leone A, Dodell-Feder D, Fedorenko E, Saxe R. 2011. Language processing in the occipital cortex of congenitally blind adults. Proc Natl Acad Sci U S A 108(11):4429-34.

Bedny M, Richardson H, Saxe R. 2015. "Visual" Cortex Responds to Spoken Language in Blind Children. J Neurosci 35(33):11674-81.

Bruel-Jungerman E, Davis S, Laroche S. 2007. Brain plasticity mechanisms and memory: a party of four. Neuroscientist 13(5):492-505.

Burton H, Snyder AZ, Conturo TE, Akbudak E, Ollinger JM, Raichle ME. 2002. Adaptive changes in early and late blind: a fMRI study of Braille reading. J Neurophysiol 87(1):589-607.

Cole MW, Pathak S, Schneider W. 2010. Identifying the brain's most globally connected regions. Neuroimage 49(4):3132-3148.

Coullon GS, Emir UE, Fine I, Watkins KE, Bridge H. 2015. Neurochemical changes in the pericalcarine cortex in congenital blindness attributable to bilateral anophthalmia. J Neurophysiol 114(3):1725-33.

Damoiseaux JS, Rombouts SA, Barkhof F, Scheltens P, Stam CJ, Smith SM and others. 2006. Consistent resting-state networks across healthy subjects. Proc Natl Acad Sci U S A 103(37):13848-53.

Everitt BJ, Robbins TW. 1997. Central cholinergic systems and cognition. Annu Rev Psychol 48:649-84.

Fine I, Park JM. 2018. Blindness and Human Brain Plasticity. Annu Rev Vis Sci 4:337-356.

Froemke RC, Merzenich MM, Schreiner CE. 2007. A synaptic memory trace for cortical receptive field plasticity. Nature 450(7168):425-9.

Gauthier CJ, Fan AP. 2019. BOLD signal physiology: Models and applications. Neuroimage 187:116-127.

Goard M, Dan Y. 2009. Basal forebrain activation enhances cortical coding of natural scenes. Nat Neurosci 12(11):1444-9.

Goldreich D, Kanics IM. 2003. Tactile acuity is enhanced in blindness. Journal of Neuroscience 23(8):3439-3445.

Gougoux F, Belin P, Voss P, Lepore F, Lassonde M, Zatorre RJ. 2009. Voice perception in blind persons: a functional magnetic resonance imaging study. Neuropsychologia 47(13):2967-74.

Gougoux F, Lepore F, Lassonde M, Voss P, Zatorre RJ, Belin P. 2004. Neuropsychology: pitch discrimination in the early blind. Nature 430(6997):309.

563 Hagmann P, Cammoun L, Gigandet X, Meuli R, Honey CJ, Wedeen VJ and others. 2008. Mapping
564 the structural core of human cerebral cortex. PLoS Biol 6(7):e159.
565 Honey CJ, Sporns O, Cammoun L, Gigandet X, Thiran JP, Meuli R and others. 2009. Predicting
566 human resting-state functional connectivity from structural connectivity. Proc Natl Acad
567 Sci U S A 106(6):2035-40.
568 Hull T, Mason H. 1995. Performance of Blind-Children on Digit-Span Tests. Journal of Visual
569 Impairment & Blindness 89(2):166-169.
570 Kanjlia S, Pant R, Bedny M. 2019. Sensitive Period for Cognitive Repurposing of Human Visual
571 Cortex. Cereb Cortex 29(9):3993-4005.
572 Kilgard MP, Merzenich MM. 1998. Cortical map reorganization enabled by nucleus basalis
573 activity. Science 279(5357):1714-8.
574 Kupers R, Pappens M, de Noordhout AM, Schoenen J, Ptito M, Fumal A. 2007. rTMS of the
575 occipital cortex abolishes Braille reading and repetition priming in blind subjects.
576 Neurology 68(9):691-3.
577 Lessard N, Pare M, Lepore F, Lassonde W. 1998. Early-blind human subjects localize sound
578 sources better than sighted subjects. Nature 395(6699):278-280.
579 Liu P, De Vis JB, Lu H. 2019. Cerebrovascular reactivity (CVR) MRI with CO2 challenge: A
580 technical review. Neuroimage 187:104-115.
581 Liu PY, Li Y, Pinho M, Park DC, Welch BG, Lu HZ. 2017. Cerebrovascular reactivity mapping
582 without gas challenges. Neuroimage 146:320-326.
583 Lowe MJ, Mock BJ, Sorenson JA. 1998. Functional connectivity in single and multislice
584 echoplanar imaging using resting-state fluctuations. Neuroimage 7(2):119-32.
585 Merabet LB, Battelli L, Obretenova S, Maguire S, Meijer P, Pascual-Leone A. 2009. Functional
586 recruitment of visual cortex for sound encoded object identification in the blind.
587 Neuroreport 20(2):132-8.
588 Mesulam MM, Mufson EJ, Levey AI, Wainer BH. 1983. Cholinergic innervation of cortex by the
589 basal forebrain: cytochemistry and cortical connections of the septal area, diagonal
590 band nuclei, nucleus basalis (substantia innominata), and hypothalamus in the rhesus
591 monkey. J Comp Neurol 214(2):170-97.
592 Mesulam MM, Mufson EJ, Levey AI, Wainer BH. 1984. Atlas of cholinergic neurons in the
593 forebrain and upper brainstem of the macaque based on monoclonal choline
594 acetyltransferase immunohistochemistry and acetylcholinesterase histochemistry.
595 Neuroscience 12(3):669-86.
596 Murphy MC, Nau AC, Fisher C, Kim SG, Schuman JS, Chan KC. 2016. Top-down influence on the
597 visual cortex of the blind during sensory substitution. Neuroimage 125:932-940.
598 Nau AC, Murphy MC, Chan KC. 2015. Use of sensory substitution devices as a model system for
599 investigating cross-modal neuroplasticity in humans. Neural Regen Res 10(11):1717-9.
600 Niemeyer W, Starlinger I. 1981. Do the blind hear better? Investigations on auditory processing
601 in congenital or early acquired blindness. II. Central functions. Audiology 20(6):510-5.
602 Norman LJ, Thaler L. 2019. Retinotopic-like maps of spatial sound in primary 'visual' cortex of
603 blind human echolocators. Proc Biol Sci 286(1912):20191910.
604 Parikh V, Kozak R, Martinez V, Sarter M. 2007. Prefrontal acetylcholine release controls cue
605 detection on multiple timescales. Neuron 56(1):141-54.

606 Pinto L, Goard MJ, Estandian D, Xu M, Kwan AC, Lee SH and others. 2013. Fast modulation of
607 visual perception by basal forebrain cholinergic neurons. Nat Neurosci 16(12):1857-
608 1863.
609 Ptito M, Moesgaard SM, Gjedde A, Kupers R. 2005. Cross-modal plasticity revealed by
610 electrotactile stimulation of the tongue in the congenitally blind. Brain 128(Pt 3):606-14.
611 Sadato N, Pascual-Leone A, Grafman J, Ibanez V, Deiber MP, Dold G and others. 1996.
612 Activation of the primary visual cortex by Braille reading in blind subjects. Nature
613 380(6574):526-8.
614 Sarter M, Hasselmo ME, Bruno JP, Givens B. 2005. Unraveling the attentional functions of
615 cortical cholinergic inputs: interactions between signal-driven and cognitive modulation
616 of signal detection. Brain Res Brain Res Rev 48(1):98-111.
617 Scholvinck ML, Maier A, Ye FQ, Duyn JH, Leopold DA. 2010. Neural basis of global resting-state
618 fMRI activity. Proc Natl Acad Sci U S A 107(22):10238-43.
619 Striem-Amit E, Cohen L, Dehaene S, Amedi A. 2012. Reading with sounds: sensory substitution
620 selectively activates the visual word form area in the blind. Neuron 76(3):640-52.
621 Turchi J, Chang C, Ye FQ, Russ BE, Yu DK, Cortes CR and others. 2018. The Basal Forebrain
622 Regulates Global Resting-State fMRI Fluctuations. Neuron 97(4):940-952 e4.
623 Van Boven RW, Hamilton RH, Kauffman T, Keenan JP, Pascual-Leone A. 2000. Tactile spatial
624 resolution in blind Braille readers. Neurology 54(12):2230-2236.
625 Voss P, Gougoux F, Lassonde M, Zatorre RJ, Lepore F. 2006. A positron emission tomography
626 study during auditory localization by late-onset blind individuals. Neuroreport 17(4):383-
627 8.
628 Voss P, Lassonde M, Gougoux F, Fortin M, Guillemot JP, Lepore F. 2004. Early- and late-onset
629 blind individuals show supra-normal auditory abilities in far-space. Current Biology
630 14(19):1734-1738.
631 Weaver KE, Richards TL, Saenz M, Petropoulos H, Fine I. 2013. Neurochemical Changes within
632 Human Early Blind Occipital Cortex. Neuroscience 252:222-233.
633 Whitfield-Gabrieli S, Nieto-Castanon A. 2012. Conn: a functional connectivity toolbox for
634 correlated and anticorrelated brain networks. Brain Connect 2(3):125-41.
635 Zaborszky L, Hoemke L, Mohlberg H, Schleicher A, Amunts K, Zilles K. 2008. Stereotaxic
636 probabilistic maps of the magnocellular cell groups in human basal forebrain.
637 Neuroimage 42(3):1127-41.
638
639